Geomorphology 296 (2017) 104–112

Contents lists available at ScienceDirect

Geomorphology

journal homepage: www.elsevier.com/locate/geomorph

Depositional processes of alluvial fans along the Hilina Pali fault scarp, Island of Hawaii

Alexander M. Morgan [a,b,*], Robert A. Craddock [b]

[a] Department of Environmental Sciences, University of Virginia, 291 McCormick Road, Charlottesville, VA 22904, USA
[b] Center for Earth and Planetary Studies, National Air and Space Museum, Smithsonian Institution, 600 Independence Avenue SW, Washington, DC 20560, USA

ARTICLE INFO

Article history:
Received 15 March 2017
Received in revised form 7 August 2017
Accepted 8 August 2017
Available online 19 August 2017

Keywords:
Alluvial fan
Hawaii
Sieve deposition
Sediment transport

ABSTRACT

A series of previously unstudied alluvial fans are actively forming along the Hilina Pali escarpment on the south flank of Kīlauea volcano on the Island of Hawaii. These fans are characterized by their steep slopes, coarse grain sizes, and lobate surface morphology. Fans are fed by bedrock channels that drain from the Ka'ū Desert, but sediment is mostly sourced from deeply eroded alcoves carved into the Hilina Pali. Examination of recent deposits indicates that the fans are dominantly constructed from gravel and larger sized sediment. Flow discharges calculated using field measurements of channel geometries and the Manning equation indicate that events inducing sediment transport are of high magnitude and occur during high intensity precipitation events, including Kona storms. The fans along the Hilina Pali appear to be a rare example of fans formed predominately from sieve lobe deposition owing to the area's high slopes, high discharge, coarse bedload, and limited supply of fine-grained sediment. Given such conditions, sieve lobe deposition can form large lobes consisting of boulder-sized material, which may have implications for the identification of depositional processes when interpreting the stratigraphic record.

1. Introduction

Alluvial fans are depositional landforms that form where a sediment laden channel exits mountainous terrain onto a lower gradient surface. The reduction of carrying capacity and lateral spreading of the channel forces the deposition of sediment into a semi-conical shape. Alluvial fans form in environments with steep topography and sufficient sediment production and fluid discharge (Blair and McPherson, 2009). They occur in all environmental settings with fluid-driven sediment flow and sharp topographic relief, occurring not only on Earth, but also Mars (Moore and Howard, 2005) and Titan (Birch et al., 2016), the two other planetary bodies known to have had surface fluid flow.

Processes that provide sediment to alluvial fans are broadly defined as either sediment-gravity processes such as debris flows, or fluid-gravity processes, which include sheetfloods and incised channel flows (Blair and McPherson, 2009). When sediment-laden flow debouches onto a permeable, coarse-grained fan surface, water may infiltrate into the fan and the coarsest material in the flow acts as a sieve, permitting water and fines to transport through while coarser grains are deposited. Hooke (1967) described this process as sieve lobe deposition, and it was once widely used in alluvial fan literature to describe such processes and their subsequent deposits (Hooke, 1967, 1968; Bull, 1972; French, 1987; Nemec and Postma, 1993). This style of deposition is particularly prevalent in settings with a scarcity of fine-grained sediment, significant bedload, and permeable ground (Nemec and Postma, 1993). Later researchers argued that such conditions do not occur in nature and that the sieve lobe model is based on the erroneous interpretation of weathered, fine-winnowed debris flow deposits (Blair and McPherson, 1992, 1993, 2009). Following Blair and McPherson's (1992, 1993, 1994, 1995, 2009) rejection of the sieve lobe model, the term fell out of usage, but has recently been revived as a fundamental process in describing alluvial fan formation and architecture (Milana, 2010; Chen et al., 2017).

In this report, we describe a series of alluvial fans along the south flank of Kīlauea volcano on the Island of Hawaii. These landforms were included in the Wolfe and Morris (1996) geologic map as Holocene and Pleistocene alluvial and colluvial fill and have been noted in previous studies (Tunison et al., 1994; Craddock et al., 2006; Craddock and Golombek, 2016), but to date have not been studied in detail. We present results from a remote sensing study and field investigation of the fans, and describe our interpretation of the fan deposits as having formed dominantly from sieve deposition associated with the region's the limited availability of fine-grained sediment and steep slopes that assist bedload transport.

* Corresponding author at: Department of Environmental Sciences, University of Virginia, 291 McCormick Road, Charlottesville, VA 22904, USA.
E-mail addresses: amm5sy@virginia.edu (A.M. Morgan), craddockb@si.edu (R.A. Craddock).

http://dx.doi.org/10.1016/j.geomorph.2017.08.028
0169-555X/

2. Geologic and climatic setting

Hawaii is the largest and most volcanically active island in the Hawaiian island chain. It is comprised of five volcanoes, the youngest of which is Kīlauea at an elevation of 1200 m. Eruptions occur both from the summit caldera and the two rift zones that radiate from the summit to the southwest and east (Fig. 1). The north flank of Kīlauea is stabilized against the much larger Mauna Loa volcano, but the south flank is unstable and is moving seaward at a rate of ~6–10 cm/yr (Owen et al., 1995, 2000), though it may move catastrophically, such as the 3 m of displacement that took place during the 7.2 M 1975 Kalapana earthquake (Lipman et al., 1985). At the surface, this slippage is manifested as two normal fault systems, the Koa'e Fault Zone and the much larger Hilina Fault System along the coast. The 42 km long, up to 5 km wide, and ~9 km deep Hilina Fault System's subaerial component is dominated by the 500 m high Hilina Pali escarpment.

Twelve distinct fan landforms exist along the base of the Hilina Pali (Fig. 2 and Table 1). The fans are fed by channels that have carved deep alcoves into the Hilina Pali (Figs. 2 and 3) and drain the Ka'ū Desert, on the leeward flank of the Kīlauea volcano. The Ka'ū Desert receives ~1300 mm of rainfall annually (Giambelluca and Sanderson, 1993), so it is not a true desert but rather a chemical desert because of sulfuric aerosol fallout from the summit caldera that inhibits vegetation growth (Schiffman et al., 2000). No weather stations record precipitation in the Ka'ū Desert, but several NOAA weather stations exist in the surrounding area (Table 2). Volcanic eruptions along the Southwest Rift Zone occur frequently, and the Ka'ū Lava Ramp is regularly resurfaced. Geologic mapping and radiometric-derived ages indicate that the oldest surfaces in the Ka'ū Desert are <750 yr old (Wolfe and Morris, 1996) and consist of lavas, splatter cones, and tephra. The Ka'ū Desert is bisected by the 10–20 m high, 12 km long, and 2 km wide Koa'e Fault Zone that connects the rift zones south of the Kīlauea summit caldera ~4 km upslope from Hilina Pali and is the smaller subaerial expression of the south flank slip. The Koa'e system as a whole is likely a long-lived feature (Podolsky and Roberts, 2008), but from lava flow stratigraphy, current rates of seaward displacement, and oral records of native Hawaiians, Duffield (1975) estimated that most of the observable displacement has occurred in the past 500 yr. The water table depth at Kīlauea summit is 490 m (Zablocki et al., 1974), and groundwater in the Ka'ū Desert is essentially nonexistent except immediately following precipitation.

The main bedrock formation exposed along the Hilina Pali escarpment is a 300 m thick portion of the Hilina Basalt, consisting of pāhoehoe and 'a'ā lava flows (95% of exposure) with interspersed ash layers (5% of exposure) (Easton, 1987). Layers of pāhoehoe and 'a'ā both show evidence for surface weathering, with the pāhoehoe lava layers having lost ~1–10 cm of material and the 'a'ā clinker zones having been partially to totally weathered to a reddish-brown clay (Easton, 1987). The Hilina Pali is overlain by the ~15 m thick, 31 ± 0.9 ka Pahala ash and the ~50 m thick, <23 ka Puna Basalt formations, which is capped by the 5–12 m thick, ~500 yr old Keanakāko'i ash (McPhie et al., 1990). The total thickness and age of the Hilina Basalt is uncertain, but ash layers near the base of the exposed lavas date from ~100 ka (Easton, 1987).

3. Methods and data

The primary remote sensing datasets we used in our analyses are a digital elevation model (DEM) with a 10 m horizontal resolution and ~5 m vertical accuracy (Sugarbaker et al., 2017) and public domain aerial orthoimagery with resolution of ~0.25 m (USGS, 2010). We define the fan apex as the location where contours shifted direction from concave (convergent flow) to convex (divergent flow), lateral fan boundaries by an abrupt end of convex form, and fan toes by the sharp change in slope and an end to convex contour orientation. We measured a number of morphometric properties, including fan size, gradient, feeder channel geometry and relief, and watershed area.

We generated longitudinal profiles using 13 points along each transect: the fan toe, five equally spaced points along the fan, fan apex, seven equally spaced points along the alcove, and the upper edge of each alcove where it met the feeder channel. We took the average elevation within a 15 m radius around each point to compensate for the roughness of the fan and alcove surface.

Feeder channels were mapped both visually using the orthoimagery and by using a D8 algorithm within ArcHydro to derive flow accumulations, extract watersheds, and discern flow paths from the DEM. The terrain is difficult to traverse, consisting of a number of overlapping, undulating older lava flows, and the area is also extensive (~30 km^2), so we did not bring heavier surveying tools such as differential GPS, which would have required establishing several

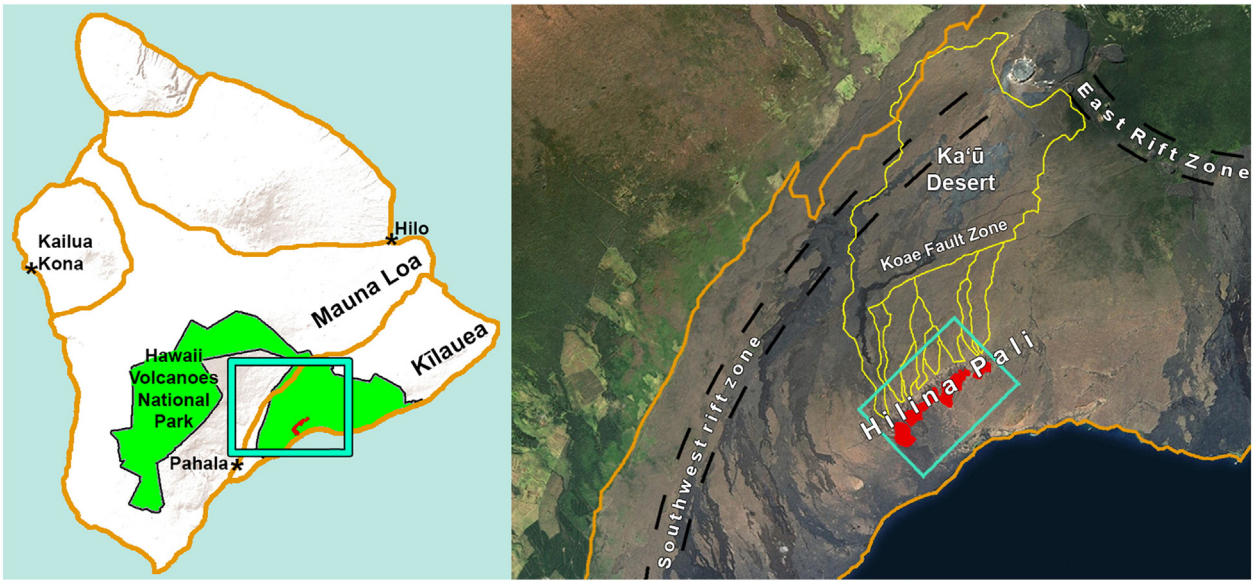

Fig. 1. Overview of study region. Left: map of the Island of Hawaii centered on 19.6°N, 155.4°W. Box indicates location of image on right. Right: Global Land Survey 2010 imagery of southeastern Island of Hawaii with features mentioned in text. Alluvial fans along the base of the Hilina Pali escarpment are outlined in red. ArcHydro-derived watersheds (see Section 3 for discussion) are outlined in yellow. The Koa'e Fault Zone directs all surface runoff from the northern Ka'ū Desert to fan F1. Box indicates the location of Fig. 2a.

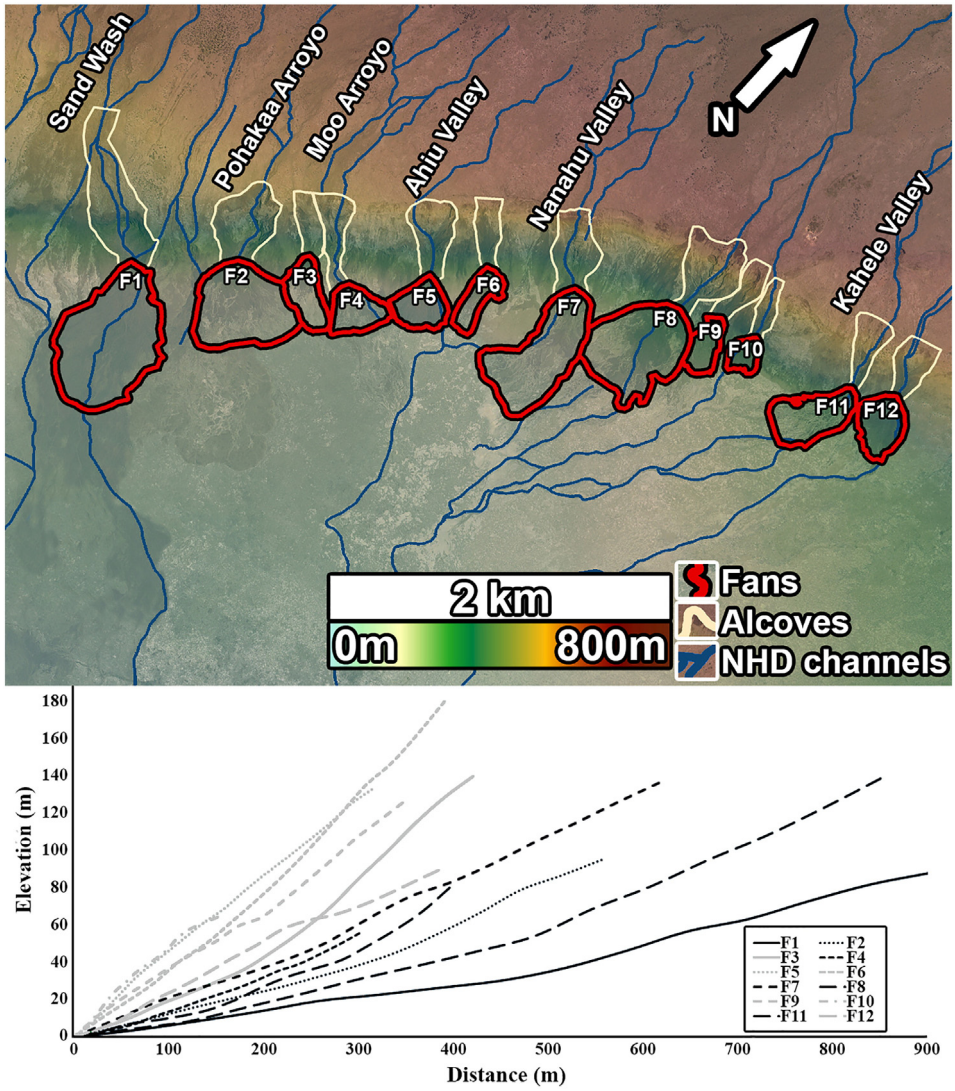

Fig. 2. Alluvial fans along the Hilina Pali escarpment. Top: map of alluvial fans and alcoves. Submeter orthoimagery overlying 10 m USGS DEM. NHD channels are those included in the National Hydrogeography Dataset. Named valleys and channels are indicated. Bottom: long profiles of fans (2× vertical exaggeration).

base stations. Every 300–500 m along the course of each channel, we measured cross sections using a measuring tape, tracking our location using handheld GPS (horizontal accuracy ~4 m). We determined surface grain size distributions by taking photographs of sediment within a one square meter area and measuring the size of each grain in Adobe Photoshop. In addition, we collected bulk samples of sediment and measured particle size distribution using standard dry sieving techniques (for sand and gravel) and laser diffraction analysis of dispersed samples.

Quantifying the flow rates and discharges responsible for the transport and deposition of fan sediment is necessary for interpreting the fan-forming processes. None of the channels are gauged, and anecdotal reports of discharges during flow events are rare. We used the Manning (1) and continuity (2) equations to estimate flow velocity U (m/s) and

Table 1
Properties of Hilina Pali fans.

Label	Name	Apex latitude (°N)	Apex longitude (°W)	Fan area (km^2)	Fan length (km)	Fan Relief (km)	Fan slope (°)	Alcove area ($km^{2)}$	Alcove relief (km)	Watershed area (km^2)
F1	Sand Wash	19.269	155.333	0.38	0.91	0.09	5.6	0.19	0.24	66.34
F2	Pohakaa Arroyo	19.273	155.329	0.27	0.56	0.09	9.0	0.23	0.31	4.67
F3	N/A	19.276	155.326	0.08	0.42	0.14	18.4	0.12	0.25	0
F4	Moo Arroyo	19.276	155.324	0.08	0.30	0.06	10.5	0.08	0.36	1.10
F5	Ahiu Valley	19.279	155.321	0.08	0.31	0.13	22.9	0.15	0.31	1.79
F6	N/A	19.282	155.319	0.06	0.39	0.18	24.7	0.08	0.32	
F7	Nanahu Valley	19.285	155.315	0.27	0.62	0.14	12.4	0.10	0.36	1.07
F8	N/A	19.288	155.309	0.28	0.85	0.14	9.2	0.11	0.35	5.80
F9	N/A	19.289	155.307	0.06	0.35	0.13	19.9	0.05	0.30	
F10	N/A	19.289	155.305	0.03	0.15	0.06	23.0	0.03	0.31	
F11	Kahele Valley	19.291	155.299	0.06	0.40	0.08	11.4	0.05	0.27	1.15
F12	N/A	19.293	155.297	0.09	0.38	0.09	13.1	0.05	0.24	3.57

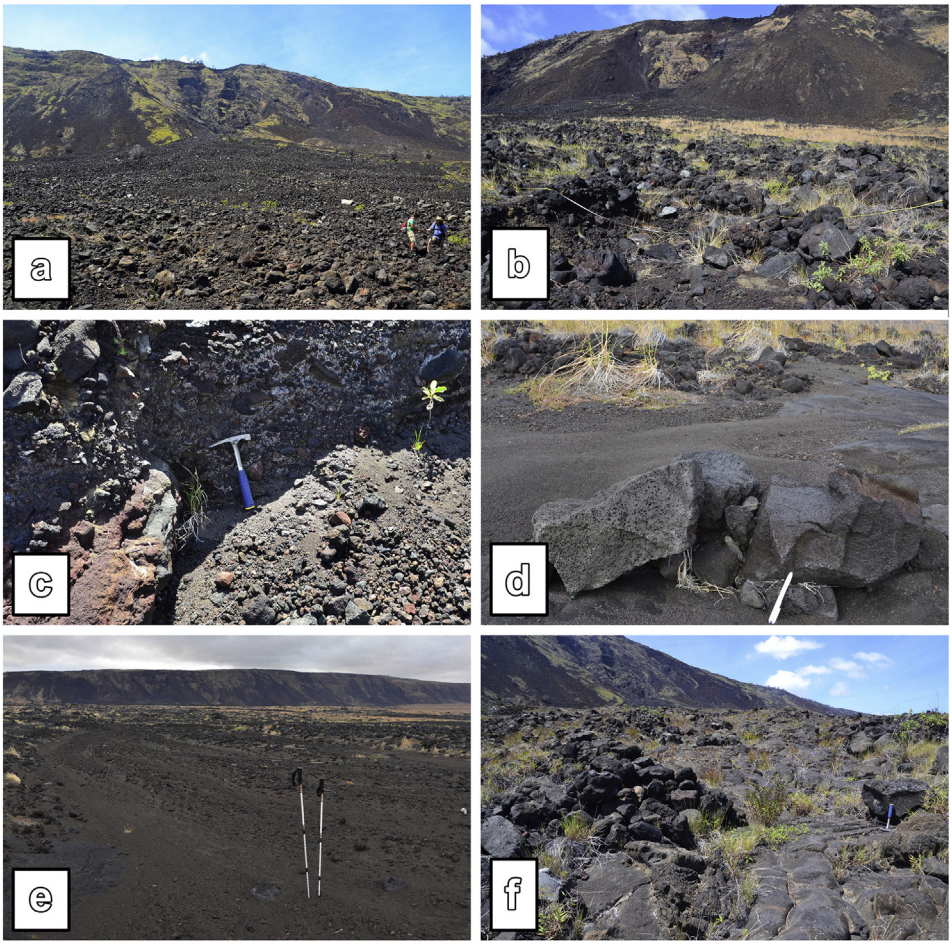

Fig. 3. Photographs of fans at the base of the Hilina Pali escarpment. Alcoves are visible at the top of (a), (b), and (f). (a) Fan F8. Large blocks, some up to a meter in diameter, make up a mantle capping the fan. (b) Levee deposits on distal portion of fan F2, note tape measure for scale. (c) Fan material at the base of a channel adjacent to a lobe. Deposits are clast supported and unlayered. Flow is to the left. (d) Imbricated clasts just downstream from the toe of fan F1, note pen for scale. Flow is to the right. (e) Gravel and sand splay near toe of fan F1. (f) Bedrock at the base of channel on distal part of fan F11. Note rock hammer for scale at center right.

discharge Q (m^3/s):

$$U = \frac{1}{n} R_h^{2/3} S^{1/2} \quad (1)$$

$$Q = UA_{XS} \quad (2)$$

where R_h is the hydraulic radius (ratio of channel cross-sectional area A_{XS} (m^2) to wetted perimeter), S is slope (m/m), and n ($s/m^{1/3}$) is the Manning-Gauckler roughness coefficient.

We used values of $n = 0.03$, 0.05, and 0.07 for the bedrock floored channels (Chow, 1959). We measured gradient using a Laser Technology TruPulse 200 rangefinder, which has $\pm 0.25°$ inclination accuracy and ± 30 cm distance accuracy. In every instance, laser rangefinder

Table 2
Weather data for the southern Kīlauea region. Distance column indicates the distance from each weather station to an approximate centerpoint of the Ka'ū Desert region (located at 19.33°N, 155.31°W, elevation 890 m).

Station	Location	Elevation (m)	Distance (km)	Years	Highest daily total precipitation (mm)		Total annual precipitation (mm)	
					Decadal average	Decadal max	Decadal average	Decadal max
HALEMAUMAU 52, HI US	19.4°N, 155.28°W	1110	8.2	1951–1959	193.8	291.1	2634.3	3687.8
				1960–1969	148.6	298.2	2630.0	3359.9
				1970–1979	60.8	238.8	2722.9	3603.5
				1980–1989	151.8	328.9	2672.1	3445.0
				1990–1999	126.1	286.0	2755.5	4657.3
				2000–2008	225.0	331.7	2793.6	3372.6
				2011–2012	NoData	NoData	1871.1	1872.0
KEALAKOMO 38.8, HI US	19.29°N, 155.14°W	110	15.5	1996–1998	NoData	NoData	1476.7	2200.4
				2004–2008	NoData	NoData	1576.9	1777.7
KAPAPALA RANCH 36, HI US	19.28°N, 155.45°W	635	18.7	1953–1955	NoData	NoData	1271.9	1470.9
				1983–1988	NoData	NoData	1247.7	1668.5
				1990–1999	NoData	NoData	1532.6	2744.2
				2000–2009	NoData	NoData	1361.9	1937.0
				2010–2010	NoData	NoData	462.5	462.5

slope measurements of channel sections were within ±2° of the values we extracted from the DEM. Our method of flow depth measurements varied between sites. In some locations, we were able to directly measure a flow depth from vegetation debris or slack water deposits at the high-water mark of channel flow, but at other areas we estimated depth by calculating the required flow shear stress necessary to transport observed sediment on the channel bed. The critical shear stress τ_c (N/m^2) required to transport sediment of diameter D (m) is:

$$\tau_c = \tau_* \left(\gamma_s - \gamma_f\right) D \tag{3}$$

where γ_s and γ_f are the specific weights (density ρ (kg/m^3) times gravity g (m/s^2)) of sediment and water, respectively, τ_* is the dimensionless boundary shear stress (Shields coefficient), and D is the grain diameter. The shear stress on the channel bed τ_b is:

$$\tau_b = \rho_f g h S \tag{4}$$

where h is flow depth (m). At the initiation of sediment motion, $\tau_b = \tau_c$. Equating Eqs. (3) and (4) yields a threshold flow depth

$$h = \left(\tau_* D\left(\rho_s - \rho_f\right)\right) / \left(S \rho_f\right) \tag{5}$$

Shields (1936) showed that a value of $\tau_* = 0.045$ is applicable to a wide range of boundary Reynolds numbers, although τ_* has been shown to vary between 0.03 and 0.06, depending on sediment sorting and particle shape (Komar, 1988), so we calculated depths at a range of values.

The primary sources for error in the above calculations are the values of flow depth, bed roughness, and slope. Channels exhibit extreme diversity in terms of roughness and amount of bedload sediment (Fig. 3c–d), and the channel course is partially defined by lava surface morphology and locations of collapsed lava tubes. We therefore used conservative values and stress that any estimates of discharge are rough approximations. Use of multiple methodologies and realistic required precipitation rates offer some check of discharge reliability.

4. Morphologic and morphometric observations

4.1. Fan observations

All the fan surfaces are dominated by a ~2 m thick mantle of boulders, cobbles, and gravels (Fig. 3a). Some boulders are up to a meter in diameter. Gravels are packed between larger grains with no interclast matrix, and there is virtually no sediment finer than coarse sand in the upper few meters. We observed little contrast in sediment size, sorting, or angularity between the proximal, medial, and distal fan regions on the higher gradient fans (those with mean surface slopes >13°), but on the lower gradient fan surfaces particles noticeably decrease in size with distance downfan. The mantle is less obvious in the distal fan deposits, but this is partially due to obscuration by a grass cover.

Viewed in aerial orthoimagery the lower gradient fans feature channels radiating from the fan apex with some degree of sinuosity, but from the ground these can be difficult to discern (Fig. 4). On the proximal fan, channel locations are defined by radially lobate deposits reminiscent of debris flow material but lacking an interclast matrix. Lobes are typically tens of meters in length, and have frontal dimensions on the order of meters. Channels contain an appreciably higher concentration of gravels than do the lobes, and sediment imbricated in relation to the flow downchannel consists primarily of poorly sorted, angular to subangular, fine gravel to cobble sediment (Fig. 3). Sediment in the channel bed of the fans was found to contain a higher proportion of finer grained (fine sand) sediment than the feeder channels (Fig. 5). In the aerial imagery, channels are <10 m wide and not generally traceable for more than ~100 m on each fan, but become more organized and discernable

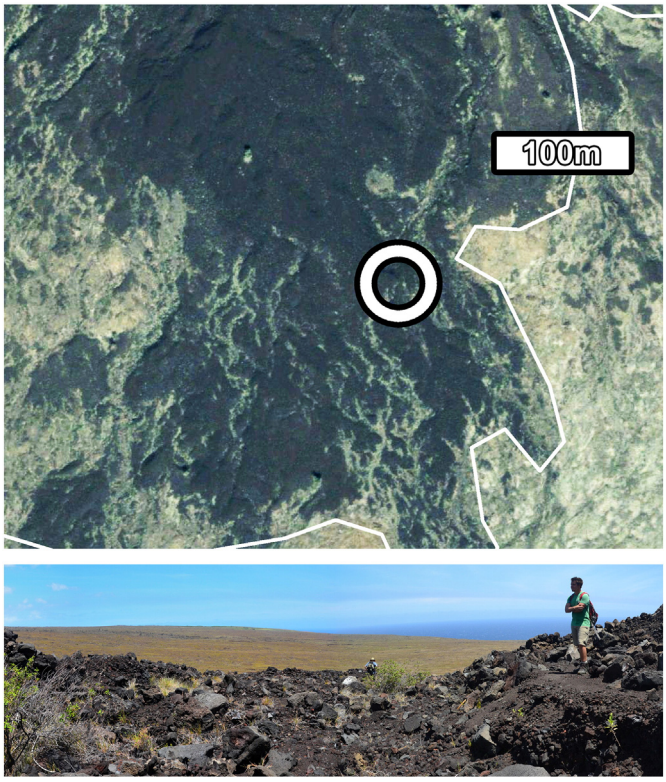

Fig. 4. Top: portion of fan F8 (outlined), north is towards the top of image. Circle indicates location of bottom photo. Note light-colored (vegetated) sinuous channels on medial to distal fan deposits. Channels are also present on the proximal fan, but are less obvious from aerial imagery due to lack of vegetation. Bottom: channel lined by lobate features, photo is looking in the downslope direction. (For interpretation of the references to color in this figure legend, the reader is referred to the web version of this article.)

past the fan toe. The exception to this is the westernmost fan F1 (see Fig. 2 and Table 1 for labeling notation) that has a main channel that can be traced from the apex to the coastline, albeit with many branches and merges. We did not observe much channel incision into previously-emplaced fan deposits, but in places channel wall exposures did reveal that below the surface boulder-cobble-gravel mantle, sediments are cemented, clast supported, medium sorted, and subangular (Fig. 3c).

The observed higher gradient fans have sharply defined toes, with very little or no sediment being transported beyond the main fan. The lower gradient fans feature levees that extend outward beyond the fan toe (Fig. 3b). These consist of gravels and cobbles with a portion of sand that increases with depth, but overall levees are largely grain supported with no interclast matrix. Beyond the fan toes, cobbles and boulders up to 30 cm diameter are imbricated in relation to the downstream direction (Fig. 3d) and splays of gravel radiate from the channels. We map these as “extended fan”, in that they consist of transported fan material but lie beyond the convex contours that define the fan.

Lava flows are stratigraphically interspersed with fan deposits. For example, fan F2 is depositing on and reworking the surface of a previously emplaced 'a'ā flow along the base of the pali, and portions of fan F11 have been covered by 'a'ā lavas. In areas fan channel floors were bedrock channel (Fig. 3f), having incised through fan material to a layer of previously emplaced lava.

4.2. Feeder channel observations

The fans are fed by ephemeral bedrock channels sourced from the Ka'ū Desert that have carved deep alcoves into the Hilina Pali above each fan, which appear to be the main sources of fan sediments. Upstream from the alcoves, channels erode into lava, ash, and layered scoria deposits (Fig. 6a). Channel beds occasionally consist of clean, smooth

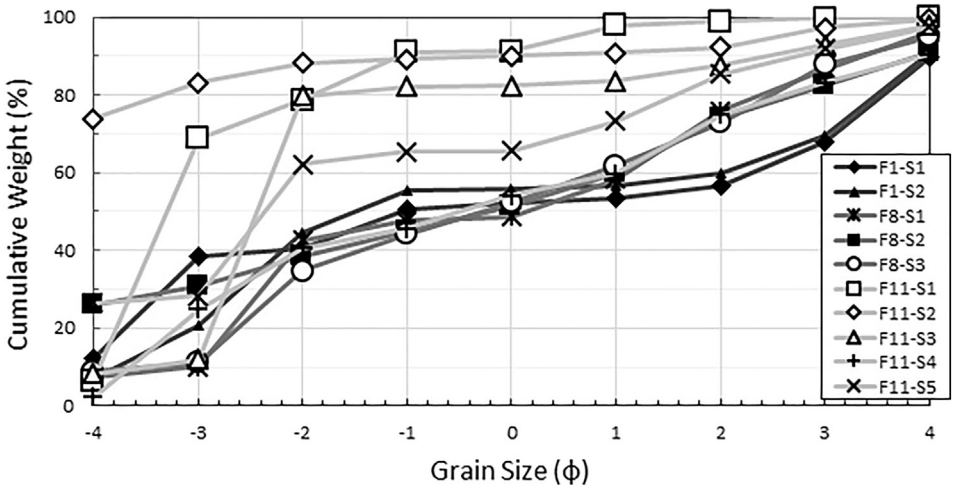

Fig. 5. Grain size cumulative curve for collected gravel and sand sized sediment. Sediment was measured at 1ϕ intervals. White markers indicate samples collected at feeder channels, black markers indicate samples collected from fan surfaces.

bedrock, but at most locations we observed grain sizes ranging from medium gravel to cobbles tens of centimeters in diameter (Fig. 6b).

The interaction of channels and lavas makes for a complicated and dynamic system. Lava flows will preferentially flow down eroded fluvial channels, and subsequently the fluvial channels will establish new pathways. Many of the channels we observed have not had time to equilibrate into the landscape, so they have very unsteady local gradients. Separating discernable channels that were primarily fluvial features from those that were primarily lava flow features was often difficult. For example, several feeder channels are located in collapsed lava tubes, and the channel feeding fan F11 is undergoing headward erosion above the main pali escarpment that appears to be driven by the emergence from a lava tube. Consequently, the drainage networks feeding the fans are poorly defined, and are generally not discernable either from aerial imagery or on the ground beyond ~2 km upstream from the main Hilina Pali escarpment. The only exception is the channel network feeding fan F1, which drains a large gully known as Sand Wash that has incised the Keanakāko'i Tephra deposit directly west of the Kīlauea summit caldera (Craddock et al., 2012). The Koa'e fault zone directs all runoff north of ~19.32°N into the channel feeding F1. Water could be transported below the surface through rock fractures and lava tubes, but the degree to which subsurface water could flow in such a manner to bypass the Koa'e fault zone is poorly constrained.

Fig. 6. Feeder channel observations. Top left: feeder channel has eroded into previously-emplaced layered scoria. Top right: imbrication of large clasts in bedrock channel feeding fan F11. Bottom: diversity in bed roughness and presence of bedload material in feeder channels. From left to right, channels range from smooth bedrock with no sediment clasts, rough bedrock with no sediment, rough bedrock with sediment (gravels and cobbles) covering channel floor, to smooth bedrock with extensive sediment on the channel bed.

4.3. Hydrology

We focused our hydrology study on fan F11, which is fed by a relatively well-organized channel network that does not intersect with the other fan drainage areas. Many of the other fans share watersheds and channels feeding the fans anastomose. In addition, F11 and its feeder channel were relatively easy to access, and the fan is similar in size, gradient, and grain size to all of the other lower-gradient fans with the exception of F1. The primary channel feeding F11 is bedrock floored with grains ranging in size from medium gravels to large cobbles, which is much smaller than much of the material present on the fan surface. Using the methods described in Section 3, we estimated channel discharges ranging from 2 to 10 m^3/s (Table 3). Multiple methods of discharge calculation yielded similar results within a half order of magnitude. Infiltration rates across most of the Ka'ū Desert are not well constrained. There is a thin (<0.25 m) sandy soil cover associated with vegetation over the region within ~1 km distance from the Hilina Pali, but the surface over most of the Ka'ū Desert is solid lava, with permeable structures such as joints and lava tubes that could either store water or transport it downslope to the Hilina Pali. Assuming near-complete runoff, our calculated discharges suggest precipitation rates of 5–30 mm/h.

4.4. Morphometry

We used an interpolation function on the DEM to estimate fan and eroded alcove volume, a comparison of which can provide an assessment of the source of fan sediment and a formative timescale. However, observations of lavas interspersed with fan deposits suggests that the estimated volume of fan sedimentary material should be treated with caution. We did find a statistically significant (at the 5% level of significance) high correlation ($R^2 = 0.86$) between fan surface areas and eroded alcove volumes, leading us to infer that sediment is dominantly sourced from the alcoves rather than transported from farther upstream. Supporting this is our observation that material comprising the fans was much larger than what we observed within the feeder channels upstream from the alcoves. We infer that the young age of the Ka'ū Desert lavas (<750 yr (Wolfe and Morris, 1996)) results in poorly organized channels that cannot effectively erode the surface, the lack of vegetation reduces weathering and transportable sediment production, and aeolian activity quickly removes or reworks any generated sediment. Upon reaching the much steeper Hilina Pali, the channel bed shear stress increases, allowing for the transport of larger sediment, and flow can more easily pluck exposed lava layers along the Hilina Pali than the smooth Ka'ū Desert lavas. Additionally, the highly-fractured lavas could possibly provide conduits for water to seep into the subsurface and travel through lava tubes before discharging at the Hilina Pali escarpment.

Researchers commonly characterize alluvial fans by the relationships between fan gradient or fan area with catchment area, basin relief, and sediment grain size (Harvey, 2011). The individual watersheds feeding each fan are not well constrained. We did not find any statistically significant relations between fan properties and watershed size, relief, or gradient, likely due to lava flows and tectonic activity constantly changing Kīlauea's surface topography. However, regression analyses indicate statistically significant (at the 5% level of significance) relationships between several morphometric parameters (Table 4). We report derived watershed areas (using ArcHydro tools on the 10 m DEM) in Table 1, but for our morphometric regression analyses we instead used the areas of the alcoves carved into the Hilina Pali. As discussed above, we believe this it is reasonable since the bulk of sediment making up the fans appears to be sourced from the eroded alcoves. The relation between basin area A_b and fan area A_f or gradient G is typically expressed as a power function, $A_f = pA_b^q$, with values for exponent q ~ 0.7 to 1.1 and constant p ~ 0.7 to 2.11 (Harvey, 2011), a range that excludes the values of $q = 1.3$ and $p = 2.9$ that we derived for the pali fans. We did not find a statistically significant relation between fan gradient and alcove area. This could be due to our use of eroded alcove rather than watershed basin for the source area, as having the entire watershed as a water source affects flood discharge and water to sediment ratios, which will have an effect on fan size and gradient. That our values lie outside the range summarized by Harvey (2011) could be due to the steep nature of the eroded alcoves not fitting well with the area-area relation. Interestingly, values for the pali fans match those obtained from measurements of alluvial fans in southern Argentina described by Milana (2010) as having been formed almost entirely from sieve lobe deposition.

5. Discussion

Our calculated runoff rates suggest heavy rains are responsible for the transport of the observed bedload sediment, which are not uncommon on southern Hawaii. Many of the largest rainfall events are associated with slow-moving, subtropical cyclones known locally as “Kona storms” (Simpson, 1952), named because the winds are often easterlies or, in other words, blow from the Kona side of Hawaii. For example, during a Kona storm on 19 February 1979 the Ka'ū Desert received over 400 mm of rainfall in a 24-h period (Kodama and Barnes, 1997). Other events that can deliver hundreds of mm/day of precipitation include cold fronts, cold-core upper troposphere toughs, and tropical systems (Kodama and Barnes, 1997). There is very little soil across much of the Ka'ū Desert, so storms would result in high runoff and channel discharge. Kona storms have been found to be responsible for initiating sediment movement and channel discharge in the continuous deposit

Table 3
Estimates of flow velocities using Eqs. (1)–(5). Depths, velocities, and discharges were calculated for a range of roughness coefficients and Shields parameters (see Section 3), and we averaged these to obtain runoff rates. The low calculated runoffs for fans F1, F2, and F8 are due to the disorganized mature of their feeder channels and the unconstrained total drainage areas. Fan F11 had the most well defined channel network.

Site	D_{84}	Slope (m/m)	Depth (m)		U (m/s)	Q (m^3/s)	Runoff (mm/h)
			Measured	Calculated			
F1–1	0.49	0.11	0.27	0.23–0.46	0.39–5.50	0.39–6.53	0.19
F1–2		0.11	0.28		0.52–1.22	0.52–1.22	0.05
F1–3		0.07	0.29		0.92–2.16	0.92–2.16	0.08
F2–1	0.25	0.02		0.77–1.54	0.84–4.77	0.84–62.0	24.22
F8–1		0.11	0.23		0.82–1.92	0.82–1.92	0.85
F8–2		0.11	0.27		0.97–2.28	0.97–2.28	1.01
F8–3	0.95	0.07		0.73–1.46	1.53–8.60	1.53–71.2	22.57
F8–4	0.26	0.02	0.44	0.81–1.62	0.24–5.08	0.24–86.7	26.98
F11–1		0.11	0.14		0.70–1.65	0.70–1.65	3.68
F11–2	0.35	0.11		0.18–0.36	0.39–4.96	0.39–7.98	13.10
F11–3	0.40	0.07		0.31–0.62	0.49–5.07	0.49–9.32	15.35
F11–4	0.35	0.02		1.09–2.18	1.30–5.52	1.30–95.3	88.59
F11–5	0.43	0.11	0.23	0.20–0.40	0.97–5.30	0.97–6.74	12.07
F11–6	0.38	0.11	0.20	0.19–0.38	0.93–4.77	0.65–4.47	8.01
F11–7	0.70	0.07	0.38	0.54–1.08	1.06–6.07	1.06–15.9	26.55

Table 4
Morphometric relations fit to the equation $Y = pX^q$, where Y is the dependent variable, X is the independent variable, p is the multiplicative coefficient, and q is the exponent. Fan surface area derived from the 10 m DEM was used as a proxy for volume (see Section 4.4). Basin properties are for the drainage basins found within ArcHydro.

Dependent variable	Independent variable	p	q	R^2	P-value
Fan area	Alcove area	2.94	1.34	0.73	0.0004
Fan area	Alcove gradient	0.36	−0.24	0.37	0.0359
Fan area	Basin area[a]	12.81	0.59	0.17	0.2131
Fan area	Basin gradient	0.07	−0.22	0.38	0.0452
Fan gradient	Alcove gradient	1.15	0.42	0.43	0.0215
Fan gradient	Fan area	0.02	−1.25	0.61	0.0028
Fan gradient	Basin relief	0.03	−0.86	0.42	0.0311
Fan surface area	Alcove volume	0.03	0.71	0.86	0.0006

[a] Fan area:basin area was not found to be statistically significant (P-value = 0.213) but is included for comparison with the fan:alcove analyses.

of the Keanakāko'i tephra located near the summit of Kīlauea (Craddock et al., 2012).

The sharply defined toes and lack of channels on the higher gradient fans are indicative of formation by rock falls. The processes responsible for constructing the lower gradient fans is more difficult to discern. In most settings, the dominantly coarse grain size, steep slopes, and low concavity of the fans would suggest an origin from debris flows (Blair and McPherson, 2009). Debris flows are common on alluvial fans due to the long timescales in between flow events during which large volumes of sediment can accumulate in the source area. Debris flows are capable of carrying larger grains than ordinary fluvial flows due to the ability of the suspended sediment to assist in sediment transport. Fine-grained particles (mud or finer) reduce permeability, trapping water within the flow and greatly increasing the internal hydrostatic pressure. Debris-flow initiation can also be affected by the distribution and angularity of larger particles, with medium to coarse sand and angular clasts hindering debris flow initiation by increasing permeability (Blair, 1999). The clearest evidence we observed for debris-flows deposits were sets of paired levees in the distal portions of fans, but these were rare, and do not appear to constitute the bulk of fan sediment. We did not find any deposits in the feeder channels or on the fans that contain a significant portion of sediments fine enough (e.g., mud or silt) to reduce permeability and initiate a transition from fluvial-dominated transport to a debris flow regime. This could be due to secondary winnowing by wind or low intensity runoff, but we also found no evidence of layering indicative of debris flows or distinctive facies within the exposed fan stratigraphy. For these reasons the lower gradient Hilina Pali fans appear to be a rare example of fans that have formed dominantly from sieve deposits. This depositional process was formally defined by Hooke (1967) as a gravelly clast supported, highly permeable, moderately sorted, lobate shaped deposit that forms when water infiltrates before reaching the fan toe. Blair and McPherson (1993) posited that such deposits have not been observed in nature and that so-called sieve lobes form from the winnowing and removal of fines from a matrix-supported debris flow by subsequent water flows. They suggested that the term should be used only to describe hypothetical deposits observed in laboratory experiments. However, Milana (2010) described a series of fans built almost entirely from sieve deposits in San Juan Province, Argentina, and inferred the required formative settings to be "a scarcity of fine sediment, significant bedload, high slope, permeable ground, and discharges moderate enough to allow infiltration." The Hilina Pali fans meet all of these conditions. The sieve depositional lobes present on these fans are somewhat larger than those described on fans in the Death Valley region or Argentina (Hooke, 1967; Milana, 2010), but this is likely due to the very large sediment size (boulders) of deposited sediment making up the lobes.

There is virtually no soil across most of the Ka'ū Desert, and the limited available sand or finer-sized sediment is primarily reworked tephra that is transported as dunes by the northeasterly trade winds to the southern Ka'ū Desert. There are multiple ash members within the Hilina and Puna Basalts exposed along the Hilina Pali, and the weathered surfaces atop 'a'ā lava flow layers have weathered to clay-sized sediment (Easton, 1987). Flow may undergo a transition to debris flows when channels erode into these formations, resulting in the observed levees. However, these layers constituted a minor fraction of the total exposure, so the fine-grained sediment constitutes only a minor component of the overall available sediment budget relative to the larger grains produced by fracturing of the lava layers.

We interpret the observed clast-supported deposits at depth as comprising the bulk of the subsurface fan material and were likely also deposited by sieve lobes. Following high intensity rainfall events, such as those associated with Kona storms, the resulting channel flows transport sediment from the eroded Hilina Pali alcoves onto the fans. The steep slopes and high discharges transport large grains onto the fans, but the reduction in gradient rapidly reduces flow competence. Large grains are deposited, creating a sieve that blocks the transport of additional sediment. Water infiltrates into the fan due to the high porosity between large grains, and the channel is choked with sediment. Over time some sand and gravel-sized sediment is transported through the fan and is deposited into the observed splays near the fan toe. Chemical weathering products of basalt, along with aeolian-transported sediment that is trapped in the coarse fan mantle, accumulates at depth in the fan, where it is cemented into a relatively impermeable layer. Water from subsequent flows carries sediment farther forward, over time building up the fans. We therefore infer that the variations in Hilina Pali fan size and gradient correspond with variations in available discharge and sediment size.

6. Conclusions

The alluvial fans in southern Hawaii are characterized by their lobate surface morphology and coarse sediment. The fans are fed by channels that drain the Ka'ū Desert, but the bulk of sediment is sourced from the Hilina Pali escarpment. The scarcity of fine grained sediment, steep slopes, and high flow discharges make this region an ideal setting for sieve lobe deposition, and the fans forming along the base of the escarpment appear to be a rare example of fans formed predominately from sieve lobe deposition. Sieve lobe deposition can occur with up to boulder sized sediment given these conditions.

There are several directions for future work at the Hilina Pali fans. Higher resolution topographic data will allow us to better assess variations in sieve lobe and channel dimensions across the fans. This can be done with differential GPS surveys or ground-based lidar (UAVs are not permitted in Hawaii Volcanoes National Park). We will conduct a systematic analysis of grain size distribution with respect to downstream and cross-longitudinal directions to determine how grain size varies with distance downstream and whether there is a grain size difference between "active" and "inactive" fan areas, as well as how grain sizes vary within depositional lobes. The fans along the Hilina Pali exhibit that given high slopes and discharges, sieve lobes can be constructed with boulder sized sediment, and further study is merited to better understand this depositional process.

Acknowledgements

The authors thank Adrian Harvey and three anonymous reviewers for their constructive comments, as well as Scott Lecce's detailed editorial corrections. This work was funded by a predoctoral fellowship awarded to A. Morgan by the Smithsonian Institution, and grant NNX14AN32G awarded to R. Craddock from NASA's Planetary Geology and Geophysics Program. The authors wish to thank Scott Rowland, Peter Mouginis-Mark, and Sarah Fagents for continuing to organize the NASA Planetary Volcanology Field Workshop in Hawaii.

References

Birch, S.P.D., Hayes, A.G., Howard, A.D., Moore, J.M., Radebaugh, J., 2016. Alluvial fan morphology, distribution and formation on Titan. Icarus http://dx.doi.org/10.1016/j.icarus.2016.02.013.

Blair, T.C., 1999. Cause of dominance by sheetflood vs. debris flow processes on two adjoining alluvial fans, Death Valley, California. Sedimentology 46, 1015–1028.

Blair, T.C., McPherson, J.G., 1992. The Trollheim alluvial fan and facies model revisited. Geol. Soc. Am. Bull. 104:762–769. http://dx.doi.org/10.1130/0016-7606(1992)104<0762.

Blair, T.C., McPherson, J.G., 1993. The Trollheim alluvial fan and facies model revisited: discussion and reply. Geol. Soc. Am. Bull. 105:563–567. http://dx.doi.org/10.1130/0016-7606(1993)105<0563:TTAFAF>2.3.CO;2.

Blair, T.C., McPherson, J.G., 1994. Alluvial fans and their natural distinction from rivers based on morphology, hydraulic processes, sedimentary processes, and facies assemblages. J. Sediment. Res. A64, 450–489.

Blair, T.C., McPherson, J.G., 1995. Quaternary alluvial fans in southwestern Crete: sedimentation processes and geomorphic evolution: discussion. Sedimentology 42: 531–535. http://dx.doi.org/10.1111/j.1365-3091.1995.tb00390.x.

Blair, T.C., McPherson, J.G., 2009. Processes and forms of alluvial fans. In: Parsons, A.J., Abrahams, A.D. (Eds.), Geomorphology of Desert Environments. Springer Netherlands, Dordrecht:pp. 413–467 http://dx.doi.org/10.1007/978-1-4020-5719-9_14.

Bull, W.B., 1972. Recognition of alluvial-fan deposits in the stratigraphic record. In: Rigby, J.K., Hamblin, W.K. (Eds.), Recognition of Ancient Sedimentary Environments. SEPM (Society for Sedimentary Geology):pp. 63–83 http://dx.doi.org/10.2110/pec.72.02.0063.

Chen, L., Steel, R.J., Guo, F., Olariu, C., Gong, C., 2017. Alluvial fan facies of the Yongchong Basin: implications for tectonic and paleoclimatic changes during Late Cretaceous in SE China. J. Asian Earth Sci. 134:37–54. http://dx.doi.org/10.1016/j.jseaes.2016.10.010.

Chow, V. Te, 1959. Open-channel Hydraulics. McGraw-Hill, New York.

Craddock, R.A., Golombek, M.P., 2016. Characteristics of terrestrial basaltic rock populations: implications for Mars lander and rover science and safety. Icarus 274:50–72. http://dx.doi.org/10.1016/j.icarus.2016.02.042.

Craddock, R.A., Irwin, R.P., Williams, R., Swanson, D., Howard, A.D., Quantin, C., Zimbelman, J.R., 2006. Topical martian field studies in the Ka'u Desert, Hawaii. Lunar and Planetary Science. vol. 37, p. 1384.

Craddock, R.A., Howard, A.D., Irwin, R.P., Tooth, S., Williams, R.M.E., Chu, P.-S., 2012. Drainage network development in the Keanakāko'i tephra, Kīlauea Volcano, Hawai'i: implications for fluvial erosion and valley network formation on early Mars. J. Geophys. Res. 117, E08009. http://dx.doi.org/10.1029/2012JE004074.

Duffield, W.A., 1975. Structure and origin, Koae fault system, Kilauea Volcano, Hawaii. U.S. Geol. Surv. Prof. Pap. 856, 1–12.

Easton, R.M., 1987. Stratigraphy of Kilauea Volcano, in: volcanism in Hawaii. U.S. Geol. Surv. Prof. Pap. 1350, 243–260.

French, R.H., 1987. Hydraulic Processes on Alluvial Fans. Elsevier Science, Amsterdam.

Giambelluca, T., Sanderson, M., 1993. The water balance and climatic classification. In: Sanderson, M. (Ed.), Prevailing Trade Winds: Climate and Weather in Hawai'i. University of Hawaii Press, Honolulu, HI, p. 126.

Harvey, A.M., 2011. Dryland alluvial fans. In: Thomas, D.S.G. (Ed.), Arid Zone Geomorphology. Wiley & Sons, pp. 333–371.

Hooke, R.L., 1967. Processes on arid-region alluvial fans. J. Geol. 75:438–460. http://dx.doi.org/10.1086/627271.

Hooke, R.L., 1968. Steady-state relationships on arid region alluvial fans in closed basins. Am. J. Sci. 266, 609–629.

Kodama, K., Barnes, G.M., 1997. Heavy rain events over the south-facing slopes of Hawaii: attendant conditions. Weather Forecast. 12:347–367. http://dx.doi.org/10.1175/1520-0434(1997)012<0347:HREOTS>2.0.CO;2.

Komar, P.D., 1988. Sediment transport by floods. In: Baker, V.R., Kochel, R.C., Patton, P.C. (Eds.), Flood Geomorphology. Wiley-Interscience, New York, pp. 97–111.

Lipman, P.W., Lockwood, J.P., Okamura, R.T., Swanson, D.A., Yamashita, K.M., 1985. Ground deformation associated with the 1975 magnitude-7.2 earthquake and resulting changes in activity of Kilauea Volcano, Hawaii. U.S. Geol. Surv. Prof. Pap. 1276 (45 pp.).

McPhie, J., Walker, G.P.L., Christiansen, R.L., 1990. Phreatomagmatic and phreatic fall and surge deposits from explosions at Kilauea volcano, Hawaii, 1790 A.D.: Keanakakoi Ash Member. Bull. Volcanol. 52:334–354. http://dx.doi.org/10.1007/BF00302047.

Milana, J.P., 2010. The sieve lobe paradigm: observations of active deposition. Geology 38: 207–210. http://dx.doi.org/10.1130/G30504.1.

Moore, J.M., Howard, A.D., 2005. Large alluvial fans on Mars. J. Geophys. Res. 110. http://dx.doi.org/10.1029/2004JE002352.

Nemec, W., Postma, G., 1993. Quaternary alluvial fans in southwestern Crete: sedimentation processes and geomorphic evolution. In: Marzo, M., Puigdefábregas, C. (Eds.), Alluvial Sedimentation. Blackwell Publishing Ltd., Oxford, UK:pp. 235–276 http://dx.doi.org/10.1002/9781444303995.ch18.

Owen, S., Segall, P., Freymueller, J., Miklius, A., Denlinger, R., Arnadóttir, T., Sako, M., Bürgmann, R., 1995. Rapid deformation of the South flank of Kilauea volcano, Hawaii. Science 267:1328–1332. http://dx.doi.org/10.1126/science.267.5202.1328 (80-.).

Owen, S., Segall, P., Lisowski, M., Miklius, A., Denlinger, R., Sako, M., 2000. Rapid deformation of Kilauea volcano: global positioning system measurements between 1990 and 1996. J. Geophys. Res. 105, 18,983–18,998.

Podolsky, D.M.W., Roberts, G.P., 2008. Growth of the volcano-flank Koa'e fault system, Hawaii. J. Struct. Geol. 30:1254–1263. http://dx.doi.org/10.1016/j.jsg.2008.06.006.

Schiffman, P., Spero, H.J., Southard, R.J., Swanson, D.A., 2000. Controls on palagonitization versus pedogenic weathering of basaltic tephra: evidence from the consolidation and geochemistry of the Keanakako'i Ash Member, Kilauea Volcano. Geochem. Geophys. Geosyst. 1. http://dx.doi.org/10.1029/2000GC000068.

Shields, A., 1936. Application of similarity principles and turbulence research to bed load movement. In: Ott, W.P., van Uchelen, J.C. (Eds.), Hydrodynamics Lab. Rep. 167. Calif. Inst. of Technol., Pasadena.

Simpson, R.H., 1952. Evolution of the Kona storm, a subtropical cyclone. J. Meteorol. http://dx.doi.org/10.1175/1520-0469(1952)009<0024:EOTKSA>2.0.CO;2.

Sugarbaker, L.J., Eldridge, D.F., Jason, A.L., Lukas, Vicki, Saghy, D.L., Stoker, J.M., Thunen, D.R., 2017. Status of the 3D Elevation Program, 2015. U.S. Geological Survey Open-File Report 2016–1196:13. http://dx.doi.org/10.3133/ofr20161196.

Tunison, J.T., Zimmer, N.G., Gates, M.R., Mattos, R.M., 1994. Fountain Grass Control in Hawai'i Volcanoes National Park 1985–1992 (Honolulu, HI).

USGS, 2010. USGS High Resolution Orthoimagery for Hawaii Volcanoes National Park.

Wolfe, E.W., Morris, J., 1996. Geologic Map of the Island of Hawaii, U.S. Geological Survey Professional Paper.

Zablocki, C.J., Tilling, R.I., Peterson, D.W., Keller, G.V., Murray, J.C., 1974. A deep research drill hole at the summit of an active volcano, Kilauea, Hawaii. Geophysical Research Letters 1 (7).